Zinc Sulfide-selenium X-ray Detector for Digital Radiography

Ji-Koon Park and Sang-Sik Kang
Department of Biomedical Engineering, College of Biomedical Science and Engineering, Inje University, Kimhae, Kyungnam 621-749, Korea

Jae-Hyung Kim, Chi-Woong Mun, and Sang-Hee Nam*
Medical Imaging Research Center, Inje University, Kimhae, Kyungnam 621-749, Korea

E-mail : pjk@drworks1.inje.ac.kr

(Received 12 August 2002, Accepted 16 September 2002)

The high bias voltage associated with the thick layer (typically 500-1000 ㎛) of selenium required to have an acceptable x-ray absorption in radiography and fluoroscopy applications may have some practical inconvenience. A hybrid x-ray detector with zinc sulfide-amorphous selenium structure has been developed to improve the x-ray sensitivity of a a-Se based flat-panel digital imaging detector. Photoluminescence(PL) characteristic of a ZnS:Ag phosphor layer showed a light emission peak centered at about 450 nm, which matches the sensitivity spectrum of selenium. The dark current of the hybrid detector showed similar characteristics with that of a a-Se detector. The x-ray sensitivity of hybrid and a-Se x-ray detector was 345 pC/cm^2/mR and 295 pC/cm^2/mR at an applied voltage of 10 V/㎛, respectively. The purpose of this study was to evaluate the pertinence of a solution using a thin selenium layer, as a photosensitive converter, with a thick coating of silver doped zinc sulfide phosphor.

Keywords : Amorphous selenium, Hybrid x-ray detector, Dark current, X-ray sensitivity

1. INTRODUCTION

In recent years, flat-panel digital X-ray detectors have been extensively developed for a medical imaging applications[1-3]. New digital detectors have many advantages such as high spatial resolution, good detective quantum efficiency (DQE), and real-time imaging acquisition without geometrical distortions. Currently, two types of detection methods have been realized in digital radiography[4]. One is an indirect conversion method, in which absorbed x-ray photons are converted to visible light in a cesium iodide (CsI) layer, and the visible light is then converted to an electrical signal by a two-dimensional photodiode array. The other is a direct detection method, in which absorbed x-ray photons are directly converted to electron-hole pairs in a photoconductor and then collected as electric charges on storage capacitors via an electric field. The storage capacitor at each pixel stores a quality of charge proportional to the incident x-ray radiation. The photoconductive materials in direct conversion systems have many functional requirements such as high x-ray absorption ratio and resistivity which can reduce a low leakage current. Low threshold energy to generate electron-hole pairs can increase the high signal noise ratio (SNR). In addition, there should be no loss of charge due to charge traps in the process of transporting a charge generated in the photoconductive layer.

New approaches have recently been carried out to develop new x-ray conversion materials[5-8]. Candidate materials are silicon (Si), amorphous selenium (a-Se), lead iodide (PbI_2), tallium bromide (TlBr) and cadnium zinc telluride (CdZnTe)[7]. Among these materials, amorphous selenium has a high resistivity ($\sim 10^{15}$) which shows a low dark current, compared with CdZnTe ($\sim 10^{10}$) and PbI_2 ($\sim 10^{12}$). However, amorphous selenium suffers from low x-ray sensitivity because it has low x-ray stopping power and a high generation energy of about 50 eV per electron-hole pair. Moreover, a-Se has the disadvantage of a high voltage exceeding 10 V/㎛, namely several kV, for collecting charges.

In this work, a hybrid detector composed of a ZnS:Ag phosphor layer and a-Se photoconductive layer was fabricated as a new x-ray detector structure to improve the low x-ray sensitivity of a-Se based x-ray detector.

The dark current and the x-ray sensitivity of the hybrid and selenium detector were measured as a function of applied voltages.

2. THEORY OF ABSORPTION

For a given area A and incident photon fluence Φ (E), the energy absorbed by the unit area of detector E_{ab} (assuming no secondary interaction, e.g., K-fluorescence reabsorption) is given by

$$E_{ab} = \sum_{E} \varphi(E) A \eta(E) \frac{\mu_{ab}(E)}{\mu(E)} E \quad (1)$$

where E is the photon energy, μ (E) and μ_{ab}(E) are the attenuation and absorption coefficients of a-Se, and η (E) is the quantum efficiency(QE) determined from:

$$\eta(E) = 1 - e^{-\mu(E) d_{Se}} \quad (2)$$

The charge signal created on the unit area, q_s, is determined by the ratio of absorbed energy per unit area Eab and the energy W needed to create an electron-hole pair in a-Se:

$$q_s = \frac{E_{ab}}{W} \quad (3)$$

The ratio between the signal and quantum noise is determined from the square root of the number of photons attenuated by the a-Se layer, which is given by $\sum_{E} \varphi(E) A \eta(E)$; thus, the charge representing the quantum noise q_{qn} at each area is given by:

$$q_{qn} = \frac{E_{ab}}{\sqrt{\sum_{E} \phi(E) A \eta(E)}} \frac{1}{W} = \frac{q_s}{\sqrt{\sum_{E} \phi(E) A \eta(E)}} \quad (4)$$

3. EXPERIMENTAL

3.1 Sample fabrication

Through experimentation, it has become evident that a 0.3-1% As addition to a-Se is sufficient to diminish the crystallization rate but has the adverse effect of creating hole traps[10]. The latter disadvantage was overcome by adding Cl in ppm amounts to compensate for the As induced traps. For fabrication of chlorinated 0.3% As:Se alloy which can be used in x-ray medical imaging, small amounts of As(0.3wt%) and Cl(30ppm) are added to enhance the conducting and thermal properties of a-Se (99.999%: Nippon Rare Metal Co.).

The photoconductive layer was prepared by the thermal evaporation of a-selenium onto ITO (Indium Tin Oxide) glass[11]. Prior to a-Se layer deposition, the ITO glass (Corning glass, 2x5 cm^2) was washed by aceton and methane, by ultrasonic sound, followed by a DI water rinse, and finally blown dry by N_2.

Typical pressure during the vacuum deposition process was $2x10^{-5}$ torr. The layer thickness was controlled by a thickness monitor gauge. The thickness of evaporated a-Se film was 50 μm for the hybrid detector and 100 μm for the a-Se detector. The temperature of the substrate was maintained at about 50 by controlling the water supply. After the formation of the a-Se layer, the transparent ITO layer with an area of 1.5x1.5 cm^2 was evaporated as an upper electrode on a-Se layer by dc sputtering apparatus. ZnS:Ag layer with a thickness of 200 μm was uniformly coated on the upper ITO glass of the hybrid detector, which is actually ZnS:Ag-coupled Se detector, by a spin coating method. Fig. 1 shows the schematic cross section of the a-Se detector and hybrid x-ray detector structure.

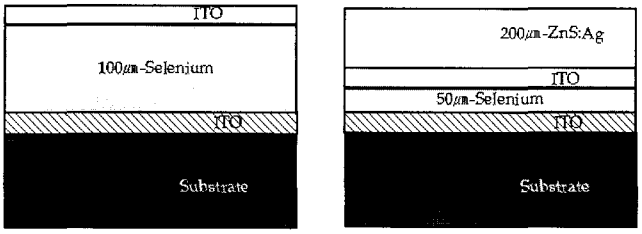

(a) (b)

Fig. 1. The schematic cross-section of (a) a-Se detector (b) hybrid detector.

3.2 Photoluminescence(PL) and light absorption

The PL measurement system is composed of a He-Cd Laser(Spirox Holding) and double monochrometer (SPEX 1403). UV light excited from He-Cd laser (55 mW) is illuminated on the surface of ZnS:Ag phosphor layer (200 μm). A photoluminescent spectrum emitted from phosphor is detected at room temperature by GaAs photomultiplier tube (R943-02) after passing through a chopper and monochrometer with diffraction grating.

The absorption spectrum of a very thin a-Se layer (1 μm) is measured by UV-VIS-NIR Spectrophotometer (Varian Cary 5E, USA). Both deuterium discharge tube for the ultraviolet(UV) region and halogen lamp for the visible-near infrared region is used as light sources, and light sources are automatically turned at about 350 nm. Detectors are composed of PM tube for the UV-Visible region and cooled PbS type cell for the near-infrared

region; the each detector is automatically exchanged at about 800 nm. The light absorption was measured at a wavelength of 200-800 nm with a scan rate of 600 nm/min.

3.3 Electrical measurement

Figure 2 shows an experimental schematic for dark current and x-ray sensitivity measurement. The experimental setup was composed of a high voltage generator (EG&G 558H, USA) for applying voltage and an Electrometer (Keithley 6517A, USA).

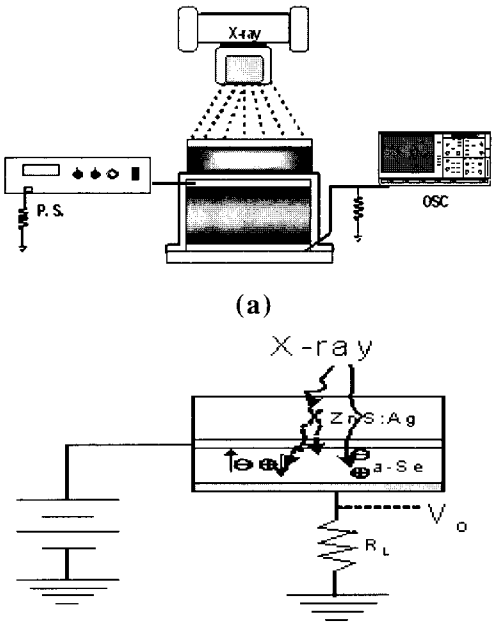

Fig. 2. Schematic diagram of x-ray sensitivity Measurement (a) Experimental Setup (b) Equivalent circuit.

I-V characteristics of the hybrid detector and a-Se detector were measured to investigate the electrical properties of both detectors. The dark currents flowing in the a-Se detector and hybrid detector were measured without x-ray irradiation during applying voltage at an interval of 2 V/㎛ from 2 to 10 V/㎛.

The experimental setup of x-ray sensitivity is similar to that of dark current except for x-ray irradiation. The X-ray generator for measuring x-ray sensitivity was a Shimadzu TR-500-125. X-ray irradiation conditions for signal acquisition were 50 kVp, 150 mA and 0.1s, respectively. The radiation dose was monitored by an Ion Chamber 2060 (Radical Cooperation, USA). After x-ray irradiation, induced voltage waveform was acquired by an oscilloscope (LeCroy, LC334A, USA). The charge was obtained by integrating an induced voltage. AcqKnowledge 3.0 was used to calculate the total charge from the waveform.

4. RESULTS AND DISCUSSION

4.1 PL emission and light absorption

Figure 3 shows the PL emission of the ZnS:Ag phosphor layer and the absorption of a very thin a-Se layer as a function of a wavelength 200-700 nm. Experimental results were obtained on ZnS:Ag (200 ㎛) and a-Se(1 ㎛) deposited on ITO glass. Photoluminescence characterization of the ZnS:Ag phosphor layer shows a broad emission peak centered at about 450 nm, which matches the sensitivity spectrum of selenium. Fig. 3 shows also the absorption of a-Se layer as a function of wavelength. Although the absorption coefficient of pure a-Se film indicates considerable absorption at a range of 2 - 3.8 eV(621 - 326 nm)[10], As and Cl doped a-Se film displays a broad absorption peak at a range of 340 -540 nm. This phenomena is actually attributable to the presence of As and Cl doped in the a-Se layer.

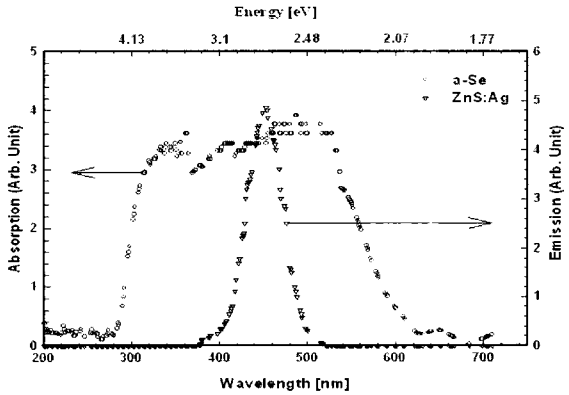

Fig. 3. PL emission of ZnS:Ag phosphor and light absorption of thin a-Se layer.

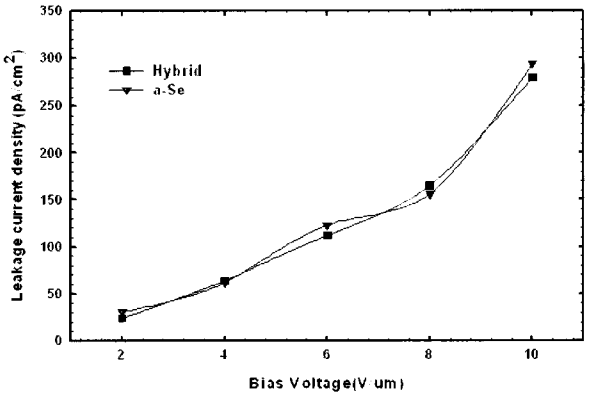

Fig. 4. Leakage currents as a function of bias electric field.

4.2 Leakage current

Even in the absence of ionizing radiation, all detectors show some finite conductivity and steady-state leakage currents are observed[12]. Fig. 4 shows the leakage currents of a-Se based detector (100 ㎛-Se) and hybrid detector (50 ㎛-Se) as a function of a biased electric field. The leakage current of the hybrid detector shows a similar behavior compared with that of the a-Se detector.

The hybrid x-ray detector displays a low leakage current of 280×10^{-8} pA/㎛^{2} at a biased electric field of 10 V/㎛. This value is twice as high as the value measured on the cesium iodide-selenium x-ray detector[6]. In the case of an amorphous semiconductor, the leakage current is due to the emission of carriers from a distribution of localized states in the energy gap[13]. It is therefore essential to significantly reduce leakage current through the use of blocking contacts. In digital x-ray imaging application, the leakage current must not exceed a few nA to avoid significant resolution degradation.

4.3 X-ray sensitivity

The interaction of incident x-ray photons with the atoms in a-Se produces an energetic primary electron which then goes on to create many electron-hole pairs. Figure 5 shows the x-ray sensitivity of the a-Se detector and hybrid detector as a function of bias voltage. The irradiation condition of the X-ray was 80 kVp, 100 mA, and 0.03 sec. The hybrid detector exhibits higher x-ray sensitivity compared with the a-Se detector (100 ㎛), especially at a higher biased electric field of 8-10 V/㎛. The X-ray sensitivities of the hybrid detector and a-Se detector were 345 pC/cm^2/mR and 295 pC/cm^2/mR at a bias electric field of 10 V/㎛, respectively.

We expect that the hybrid x-ray detector can simultaneously utilize the electric signal in a-Se layer by light absorption as well as by direct x-ray absorption. In addition, the hybrid x-ray detecting system has a potential capability for improving the thickness and, therefore, high voltage of the a-Se layer since a direct a-Se based x-ray detector uses a thick a-Se layer (typically 500-1000 ㎛) and an extremely high electric field of above 10 V/㎛, namely several kV, for collecting charges.

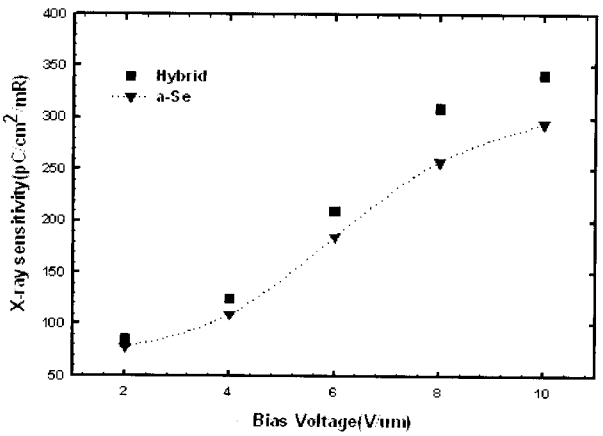

Fig. 5. X-ray sensitivity as a function of bias electric field.

4.4 Output charge

In Fig. 6, the output charges of the a-Se detector and hybrid detector are plotted as a function of the mR exposure value used, both for the hybrid detector and selenium based detector. An applied electric field was fixed at 10 V/㎛ for both samples. The output charges are linearly increasing with the energy of incident x-rays.

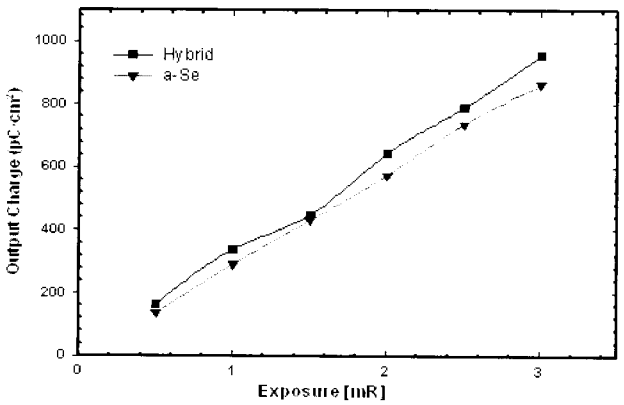

Fig. 6. Output charge versus Exposure.

5. CONCLUSION

The hybrid detecting system composed of a conventional a-Se detector and phosphor layer was fabricated to enhance electron-hole pairs generated in a-Se based x-ray detector. The hybrid detecting system utilized the electric signal generated from both electron-hole pair in photo-receptor layer and a visible light in phosphor layer simultaneously. Photoluminescence characteristics of ZnS:Ag phosphor showed a light emission peak centered at 420 nm, which matches the spectral sensitivity of a-Se based x-ray receptor of selenium.

It was also verified that the hybrid x-ray detector generated a higher electric signal compared with a conventional direct x-ray detector. This effect is due to simultaneous detection of electric signals induced by both direct x-ray absorption and light absorption in the phosphor layer. Hybrid x-ray detectors can also accumulate higher electrical signals than conventional digital x-ray detectors. In addition, the new hybrid x-ray has the added capability of improving the thickness problem of a-Se (usually, a several hundred ㎛) and the

voltage (usually, 10V/㎛) problem of a direct a-Se based x-ray detector. To improve the performances of digital x-ray detectors, further work is needed to evaluate the reduction of leakage current and to optimize the thickness of phosphor and a-Se.

ACKNOWLEDGEMENTS

This work was supported by National Research Laboratory program (M1-0104-00-0149), Korea.

RERFERENCES

[1] J. A. Rowlands and D. M. Hunter, "X-ray imaging using amorphous selenium: Photoinduced discharge (PID) readout methods for digital general radiography", Med. Phys., Vol. 18, p. 1983, 1995.

[2] W. Que, and J. A. Rowlands. "X-ray imaging using amorphous selenium: inherent spatial resolution", Med. Phys., Vol. 22, No. 4, p. 365, 1995.

[3] Wei Zhao, J. A. Rowlands, W. G. Ji, and A. Debrie, "Imaging performance of amorphous selenium based flat=panel detector for digital mammography", proc. of SPIE, Vol. 4320, p. 536, 2001.

[4] S. Tokuda, S.Adachi, T. Sato, T. Yoshimura, H. Nagata, K. Uehara, Y. Izumi, O. Teranuma, and S. Yamada, "Experimental evaluation of a novel CdZnTe flat-panel X-ray detector for digital radiography and fluroscopy", proc. of SPIE, Vol. 4320, p. 140, 2001.

[5] H. J. Lee, K. T. Lee, S. G. Park, U. S. Park, and H. J. Kim, "Electrical and leakage current characteristic of high temperature polycrystalline silicon thin film transistor", J. of KIEEME(in Korean), Vol. 11, No. 10, p. 918, 1998.

[6] Alain Jean. Luc Laperriere, Anne Legros, Habit Mani, Ziad Shukri, and Henri Rougeot, "New cesium iodide-selenium x-ray detector structure for digital radiography and fluoroscopy", proc. of SPIE, Vol. 3659, p. 298, 1999.

[7] H. Hermon, M. Schieber, A. Zuck, A. Vilensky, L. Melehov, E. Shtekel, A. Green, O. Dagan, S.E. Ready, R.A. Street, E. S. Seppi, R. Pavlyuchkova, G. Virshup, G. Zentai, and L. Partain, "Deposition of thick films of polycrystalline mercuric iodide x-ray detectors, proc. of SPIE, Vol. 4320, p. 133, 2001.

[8] S.-S. Kang, J.-H. Kim, H.-W. Lee, C.-W. Mun, and S.-H. Nam, "X-ray response characteristic of Zn in the polycrystalline $Cd_{1-x}Zn_xTe$ detector for digital radiography", Trans. on EEM, Vol. 3, No 2, p. 28, 2002.

[9] Wei Zhao and J. A. Rowlands, "X-ray imaging using amorphous selenium: feasibility of a flat panel self-scanned detector for digital radiology", Med. Phys., Vol. 22, p. 1595, 1995.

[10] A. S. Diamond, "Handbook of Imaging Materials", Marcel Deker, p. 352, 1991.

[11] H. H. Kim, M. J. Cho, W. J. Choi, J. G. Lee, and K. J. Lim, "Figure of merit for deposition conditions in ITO films", Trans. on EEM, Vol. 3, No 2, p. 6, 2002.

[12] G. F. Knoll, "Radiation detection and measurement", John Wiley & Sons, Inc., p. 368, 2000.

[13] S. O. Kasap and J. A. Rowlands, "Photoconductor selection for digital flat panel x-ray imaging detectors based on the dark current", J. Vac. Sci. Technol. A, Vol. 18, No. 2, p. 615, 2000.